International Journal of Medical Physics, Clinical Engineering and Radiation Oncology, 2023, 12, 84-97
https://www.scirp.org/journal/ijmpcero
ISSN Online: 2168-5444
ISSN Print: 2168-5436

Field Size Evaluation with a High Resolution 2D Diode Array for Variable-Aperture Collimators Used in Robotic Radiosurgery

Xiaofeng Zhu[1], Wei Nie[1], James David George[1], Qianyi Xu[1], Dandan Zheng[2*], Jiajin Fan[1]

[1]Inova Schar Cancer Institute, Fairfax, Virginia, USA
[2]University of Rochester Medical Center, Rochester, NY, USA
Email: *nedm873@gmail.com

How to cite this paper: Zhu, X.F., Nie, W., George, J.D., Xu, Q.Y., Zheng, D.D. and Fan, J.J. (2023) Field Size Evaluation with a High Resolution 2D Diode Array for Variable-Aperture Collimators Used in Robotic Radiosurgery. *International Journal of Medical Physics, Clinical Engineering and Radiation Oncology*, **12**, 84-97.
https://doi.org/10.4236/ijmpcero.2023.123008

Received: June 20, 2023
Accepted: August 7, 2023
Published: August 10, 2023

Abstract

Robotic radiosurgery/Radiotherapy is increasingly adopted in clinics, and quality assurance (QA) of CyberKnife's variable-aperture Iris™ collimators requires sub-millimeter precision. Conventional film-based QA for the 12 Iris™ cone sizes (ranging from 5 to 60 mm) is both time consuming (120 minutes for all or 30 minutes for 3 cone sizes) and highly experience dependent. To improve the efficiency, a high-resolution 2D diode detector array, sampling every 2.5 mm, was evaluated for Iris™ aperture size QA. This study focused on a spatial frequency analysis, a dose profile reconstruction, and a sensitivity study to beam size variances. Dose profiles of the 12 cones scanned with a high-resolution diode in a water tank were utilized as the gold standard for comparison. Spatial Fourier transform of these profiles were analyzed to explore applicable sampling frequency. Next, the dose profiles were artificially sampled with a 2.5 mm gap, and then interpolated using a Python-based cubic B-spline. Finally, sensitivity of the diode array system to various field sizes was measured by changing source to detector distance. We found, utilizing the diodes system, QA time was reduced to less than 10 minutes. Spatial frequency of the dose profile showed little contribution beyond 0.2 mm^{-1}, so a Nyquist sampling of 0.4 mm^{-1} is appropriate for dose verification, corresponding to a 2.5 mm gap. Dose profiles were reconstructed using Cubic B-spline with good agreements to nominal for cones 7.5 mm and larger. The measured Iris™ size using the SRS MapCheck had a standard error of ±0.12 mm. Primarily, the 2D Diode array with a spatial resolution 0.4 mm^{-1} is appropriate for dose verification for these cones above 7.5 mm, and its application would substantially improve Iris™ QA efficiency.

Keywords

CyberKnife, Diode Array, QA, FFT

1. Introduction

Using high radiation doses delivered to small tumors in one or a few fractions, stereotactic radiosurgery (SRS) and stereotactic body radiation therapy (SBRT) is capable of increasing tumor cure and reducing normal tissue toxicity [1]. Currently, SRS/SBRT is widely utilized with increasing popularity as a dominating treatment modality for intracranial and extracranial metastases. In these treatments, high doses are delivered within sub-millimeter spatial accuracy using many small radiation fields. Compared with conventional radiotherapy, higher quality assurance (QA) standards are implemented for SRS/SBRT to safeguard its more demanding spatial and dosimetric accuracy [2]. ASTRO and ACR guidelines state "strict protocols for quality assurance (QA) must be followed in SRS/SBRT" [3]. As technology advances and regulatory requirements become more stringent, it is imperative to expedite efforts towards achieving a harmonious balance between accuracy and efficiency.

Combining real-time x-ray image guidance with robotic technology, the CyberKnife (CK) system™ (Accuray, USA) is a popular system for SRS and SBRT. By mounting a miniature x-band linear accelerator on a high-precision robotic arm, CK delivers 6 MV flat-filter-free (FFF) photon beams with a high dose rate up to 2000 MU/minute. In addition to fixed SRS cone, CK's variable aperture Iris™ collimator allows for a more versatile and efficient SRS/SBRT delivery. As depicted in **Figure 1**, similar to the adjustable opening in an optical camera, in Iris™ the radiation beam aperture is shaped remotely by the collimator to deliver optimized conformal dose to the tumor. This collimator consists of 2 hexagonal banks of tungsten segments, upper and lower stacked together to produce a 12-sided aperture, with a sketch design shown in **Figure 1(b)**. Using the automated Iris™ collimators system, the circular radiation beam apertures from the CK Linac were approximated with regular dodecagons of various cone sizes. This Iris™ system consists of 12 discrete cone sizes, ranging from 5, 7.5, 10…to 60 mm, respectively. Periodical QA on the Iris™ system is essential for this high-precision, variable-aperture system. However, conducting QA becomes challenging due to the intricate nature of small-field dosimetry. This challenge

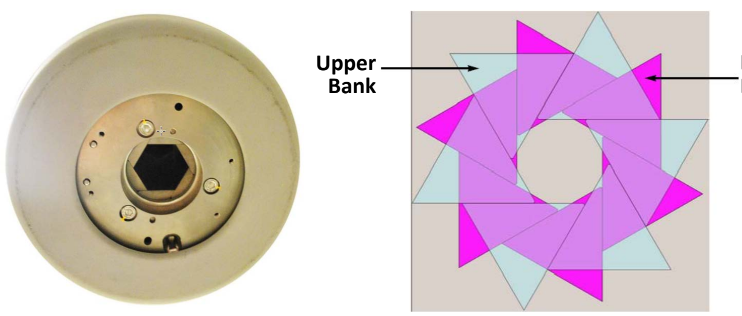

(a) (b)

Figure 1. (a) A photo of the CK Iris™ collimator; (b) a schematic plot of the Iris™ collimator, beam shape is collimated with two banks (upper and lower) of tungsten segments.

stems from various factors, including the detector volume averaging effect, the absence of lateral charged particle equilibrium, the presence of steep horizontal dose gradients, and the elevated dose rate of the Flattening Filter Free (FFF) beam [4] [5].

The conventional dosimetric QA system of choice for the CK Iris™ is the radiochromic film (Ashland, USA), which is also recommended by the CK vendor. In addition to having a high spatial resolution, film is a water tissue equivalent material which provides radiation response that is independent of beam energies. However, film dosimetry is complex and effort-consuming. For example, film response to dose fluctuates with the film batches, and is affected by the film polarization orientations. Scanning conditions, the time gap between the irradiation and the readout, and many other factors all affect the accuracy of film dosimetry. As a result, film-based QA can be quite time-consuming and expertise-dependent. For the Iris™ film-based QA, each cone field size takes about 10 minutes. For making QA tasks manageable, most clinics sample only 3 out of the 12 cones in routine monthly QA.

Similar to the measurement for patient-specific QAs, high resolution electronic QA devices have been explored to replace film in Iris™ machine QA. There are various candidate systems: SRS MapCheck is a diode-array with a resolution of 2.5 mm (Sun Nuclear Corp, Melbourne, FL), as is a replacement of the earlier SRS Profile system with a spatial resolution of 4 mm; Octavis 1000 SRS is a liquid-filled ionization-chamber array with a resolution of 2.5 mm (PTW, Germany) [6]; Octa is a 2nd generation monolithic silicon-diode array with a resolution of 0.3 mm (Univ. of Wollongong, Australia) [7]; and QA StereoChecker is a portal dosimetry type scintillator-amorphous silicon detector with a resolution of 0.3 mm (Standard Imaging). Intuitively, high resolution is important for SRS QAs. At the same time, the total number of detectors increases as a power of two with the resolution for 2D detector arrays, and the cost will increase. It remains unclear what detector resolution is sufficient for the CK Iris™ QA, to achieve a sub-millimeter accuracy.

This study aims to assess the suitability of the SRS MapCheck system as a substitute for radiochromic film in monthly CK Iris™ field size QA: The spatial frequency distribution of CK beam profiles was analyzed using Fast Fourier Transformations (FFT). A comparative analysis was then conducted, comparing dose profiles and reconstructions obtained through cubic B-spline interpolation for beams of different sizes. The primary objective was to determine the limitations in applicability resulting from detector sampling resolution of 2.5 mm. Additionally, the impact of beam size variations was evaluated by increasing the source-to-detector distances to measure the system's sensitivity in achieving sub-millimeter accuracy.

2. Methods

In this study, the suitability of the SRS MapCheck (Sun Nuclear Corp, Melbourne, FL) for the CK Iris™ field size QA was explored. The SRS MapCheck has a 2D detector array consisting of 1013 n-type solid-state diodes, sandwiched by two pieces of rectangular polymethyl methacrylate (PMMA) blocks. A CT image shows the diode array in Figure 2(a). Each diode has a measurement area is $0.48 \times 0.48\ \text{mm}^2$ and a thickness of 0.03 mm, yielding an active measurement volume of $0.007\ \text{mm}^3$. The distance between the diode center is 2.5 mm, corresponding to a spatial sampling frequency of $0.4\ \text{mm}^{-1}$. A sketch plot is presented in Figure 2(b), overlaid with a dose profile of CK Iris™ = 7.5 mm beam.

2.1. Theoretical Exploration of Sampling Frequency

In order to evaluate the CK Iris™ QA by the SRS MapCheck, the output factors and dose profiles of various Iris™ sizes from the CK commissioning data were first analyzed to investigate the impact of detector sampling frequency for generic detectors. The commission data were originally measured with a 3-D water scanning tank (MP3-M Phantom Tank, PTW, Freiburg, Germany) and a diode detector (60018 Diode, PTW, Freiburg, Germany). The dose computing inside the CK treatment planning system was built by modeling the commissioning data. The gradient of output factor changes as a factor of Iris™ aperture size, computed between adjacent cone sizes. Also, the spatial frequency of the commissioned 1D dose profiles were analyzed using a spatial Fourier transform, Equation (1), to find applicable sampling frequency.

$$F_k = \sum_{n=0}^{N-1} D_n * e^{-i2\pi kn/N} \tag{1}$$

where N = number of space samples during commissioning; D_n = value of the diode signal at space n; F_k = amount of frequency k in the signal.

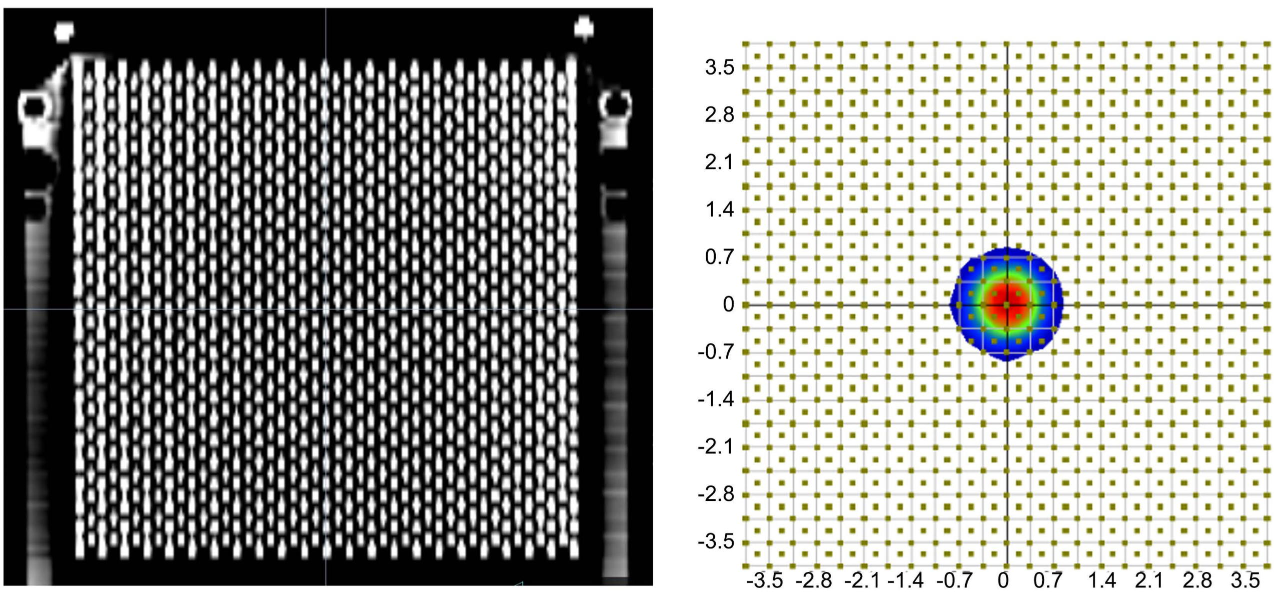

(a) (b)

Figure 2. Example of a figure caption (figure captin). (a) SRS MapCheck 2D detector array shows in CT images. (b) Sketch of the detector array with a spatial resolution of 2.5 mm measuring a 7.5 mm of Iris™ beam.

2.2. SRS MapCheck Measurements of Field Size

Subsequently, the CK Iris^{TM} field sizes were measured with the SRS MapCheck, with the experimental setup shown in **Figure 3**. The SRS MapCheck was flatly positioned on a robotic couch, with its diode detector center vertically aligned with the CK Linac gantry, with a source to detector distance (SDD) of 80 cm. The alignment process consists of two steps. First, the map check was aligned with an in-room laser system and visually verified with a naked eye, ensuring an accuracy of 2 mm. Second, the alignment was further refined using the CK two orthogonal X-ray systems and verified by 4-fiducials integrated within the SRS MapCheck detector, resulting in an improved accuracy of 1 mm.

From the SRS MapCheck, diode measurement along the two orthogonal and the two diagonal axes were collected and averaged to generate a 1D dose profile. From the 1D profile, the Iris^{TM} field size was measured at a full width of half maximum.

Using a cubic B-spline interpolation, each 1D dose profile was reconstructed from the diode measurements along the sampling axis. The SNC software, purchased with SRS MapCheck, is a "black-box" solution designed for the field size measurement. Due to proprietary reasons, there is no access to the reconstructed profile data using the commercial software. Therefore, we developed an in-house Python Scripting. Using the Scripting, the individual diodes were sorted by their distances to the beam center. Next, a cubic polynomial function described in Equation (2) was employed to interpolate a continuous curve connecting the measurement points:

Figure 3. Setup of the CK Iris^{TM} QA using the SRS MapCheck.

$$D_n(x) = a_n x^3 + b_n x^2 + C_n x + d_n, \quad (2)$$

where for the n[th] diode, its distance to the beam center is denoted as x_i, and the diode measurement is $D_n(x)$. Smoothness and continuity of the curve across the diodes was maintained by equalizing the first (Equation (3)) and second derivatives (Equation (4)) at the sampling diode locations:

$$\frac{\mathrm{d}}{\mathrm{d}x} D_{n-1}(x) = \frac{\mathrm{d}}{\mathrm{d}x} D_n(x), \quad (3)$$

$$\frac{\mathrm{d}^2}{\mathrm{d}x^2} D_{n-1}(x) = \frac{\mathrm{d}^2}{\mathrm{d}x^2} D_n(x). \quad (4)$$

The interpolated curves were overlaid with the commissioning data, to examine the correlation between the commissioning and SRS MapCheck Data. The applicability of this method to utilize SRS MapCheck measurements for CK Iris™ field size QA was evaluated by comparing the differences between the commission data and the fitted measurement data.

2.3. SRS MapCheck Field Size Sensitivity

To study the sub-millimeter resolution of the SRS MapCheck, its sensitivity to the Iris™ field size variation was studied. Because the Iris™ system cannot be programmed with intentional field size variances, measurements were made by manually changing the source to detector distances (SDDs). For each cone, all Iris™ field sizes were measured with a range of SDDs at 75, 76, …, and 85 cm, respectively. Because the projected Iris™ field size on the detector surface is proportional to the SDD, these setup configurations correspond to the change of nominal field size, respectively. Each Iris™ beam with 100 MU was delivered sequentially. The time gap between next Iris™ beams was <5 seconds. Using a SNC Patient QA software, these measured profiles were saved into one movie file. The Patient QA software was capable of extracting each Iris™ beam profile. With Cubic B-Spline interpolation built in, this QA software provided a one-click approach for the Iris™ field size measurements.

3. Results

3.1. Relative Output vs Field Size

The dose output factor for various Iris™ cone sizes were measured by SRS MapCheck after diode calibration. The relative output factor increases with the Iris™ cone size, as shown by the red dots in **Figure 4**. The green dots in **Figure 4** show the computed gradients of output factor over cone size. For Iris™ sizes larger than 10 mm, the output factors are above 0.9, and increase slowly with the Iris™ size at output gradients < 2%/mm. For the Iris™ size of 10 mm, the output factor is about 0.85, with an output gradient about 3%/mm. As Iris™ field size further decreases from 7.5 mm to 5 mm, the output factor decreases from 0.78 to 0.54, corresponding to output gradients around 10%/mm for Iris™ size < 10 mm.

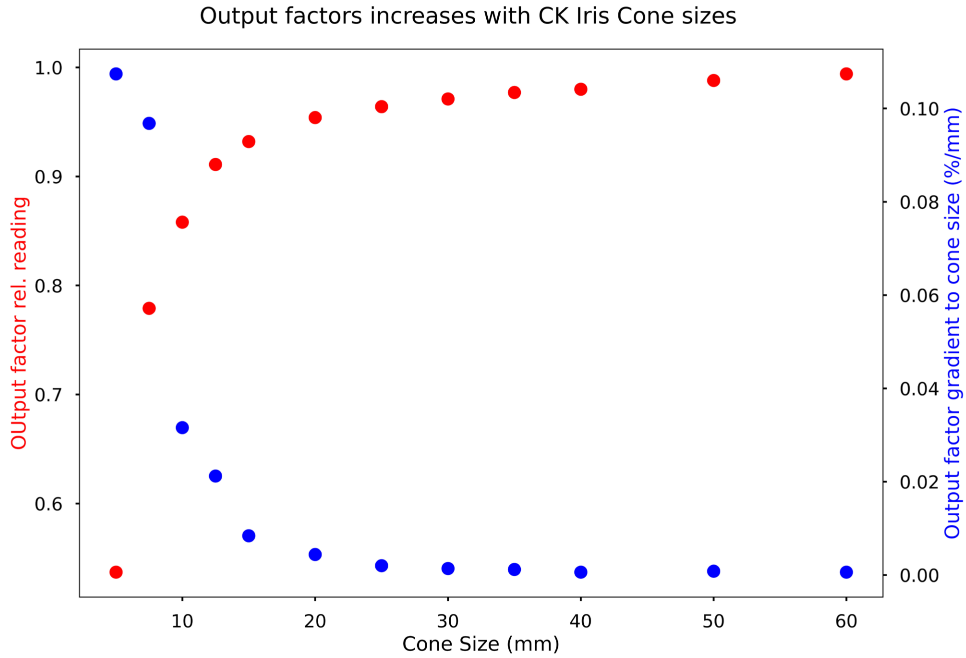

Figure 4. The relative output factor (red dot) increases with the Iris^{TM} cone size; the output factor gradient (green dot) decreases with the cone size and approaches zero for Iris^{TM} cone size > 12.5 mm.

3.2. FFT Analysis of Dose Profile

The 1D dose profiles for CK Iris^{TM} beams commissioning, scanned with a 3D water tank, are presented in **Figure 5(a)**. As the cone sizes decrease from 60 mm to 5 mm, the beam profiles change from bell-shaped to Gaussian shaped curves. FFTs of those dose profiles are plotted in **Figure 5(b)**, from which it can be observed that the majority of the signal is at spatial frequencies < 0.2 mm^{-1}. However, for Iris^{TM} sizes smaller than 10 mm, noticeable high frequency components are also observed as shown in the zoomed-in plot in **Figure 5(c)**. For instance, the 2nd peak of the FFT component appears from 0.1 to 0.2 mm^{-1} for Iris^{TM} = 10 mm; from 0.13 to 0.26 mm^{-1} for Iris^{TM} = 7.5 mm; from 0.2 to 0.4 mm^{-1} for Iris^{TM} = 5 mm, showing the largest expansion.

3.3. Cubic B-Spline Interpolation

As the FFT analysis above showed the existence of high frequency components in small cone-size beams, the 1D beam profiles were inspected further overlaying the Cubic B-spline interpolation from the 2.5 mm sampling from the water tank-scanned dose profile for Iris^{TM} sizes = 5, 7.5 and 10 mm, respectively. As plotted in **Figure 6(a)**, in general, the 2.5 mm sampled profiles agree well with the tank-scanned profiles. However, small discrepancies are also observed, especially for the smallest size Iris^{TM} = 5 mm. These profile differences are plotted in **Figure 6(b)**. It could be seen that for the 5 mm Iris^{TM} size, ~2.5% maximum difference was observed at distance 1.7 mm from the beam center. The maximum difference was 0.6% at the off-axis distance of 4 mm for the Iris^{TM} = 7.5 mm, and

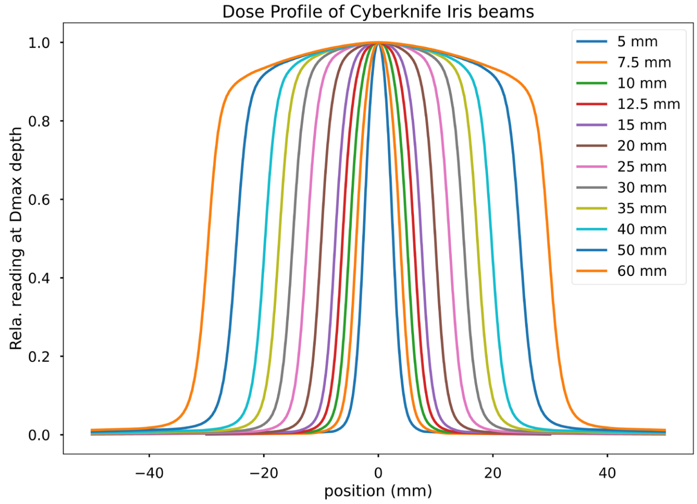

(a)

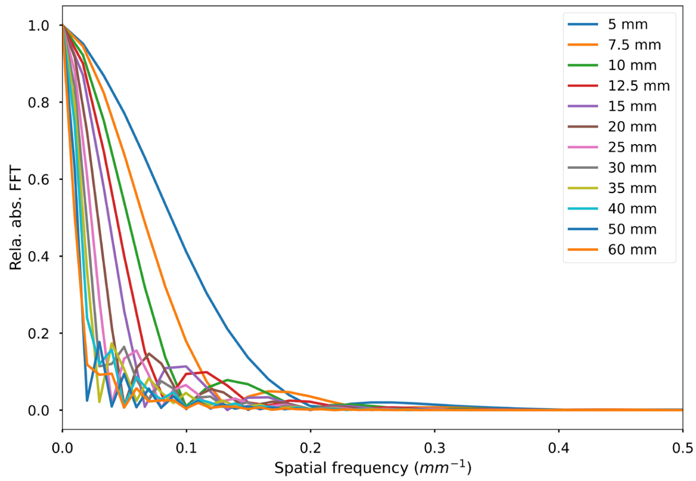

(b)

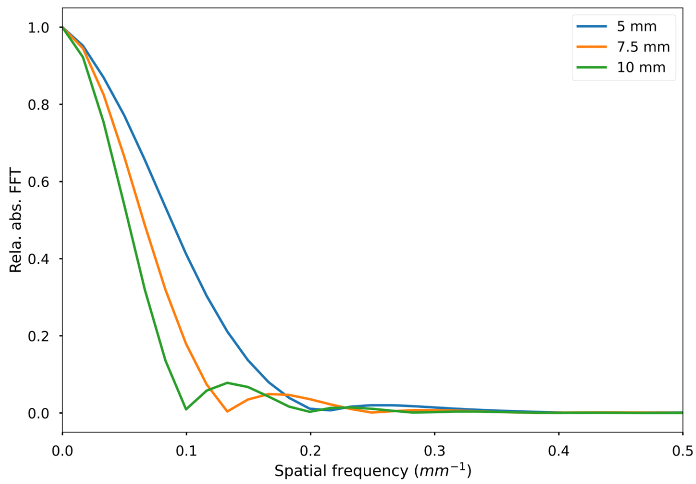

(c)

Figure 5. (a) 1-D dose profile of various CK Iris^{TM} sizes; (b) Fourier transform of the dose profiles; (c) Zoomed-in view of Fourier transform of the dose profiles for Iris^{TM} sizes at 5, 7.5, and 10 mm.

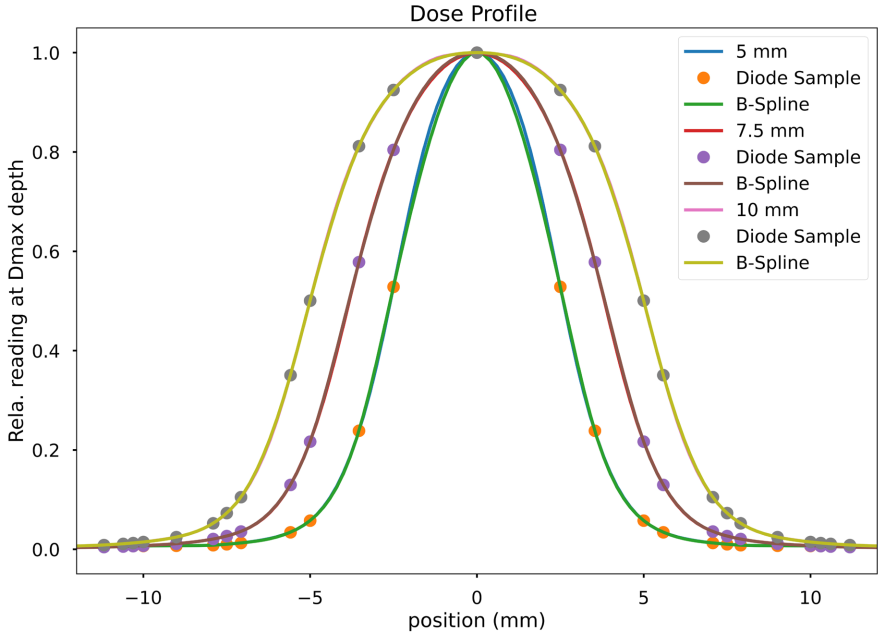

(a)

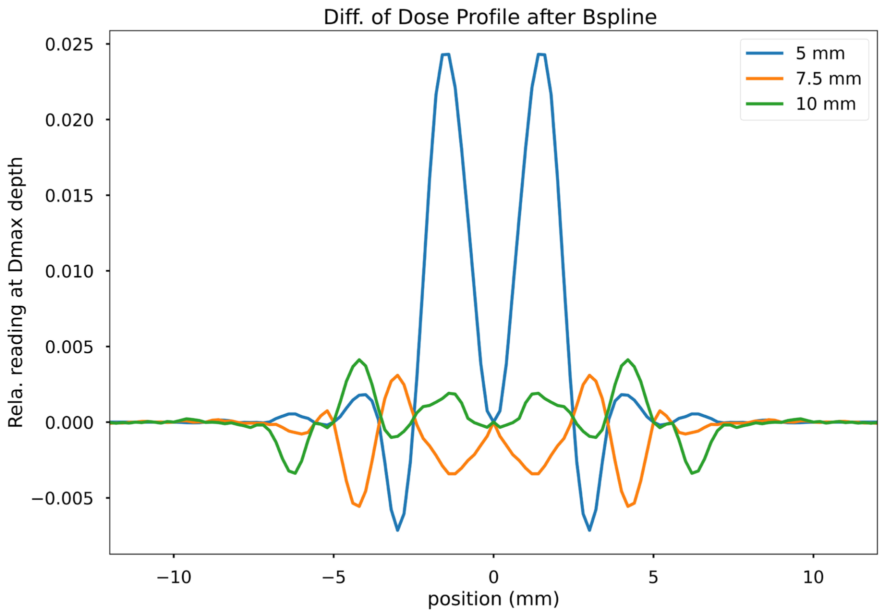

(b)

Figure 6. For Iris™ sizes = 5, 7.5 and 10 mm, (a) the profile overlays and (b) profile differences are displayed comparing the interpolation using 2.5 mm sampling with the water tank-scanned.

0.4% also at 4 mm for the Iris™ = 10 mm. In order to limit the measured dose difference smaller than 2% during SRS/SBRT, SRS MapCheck using the cubic B-spline should only be recommended for Iris™ ≥ 7.5 mm in the clinic.

3.4. Accuracy of Iris Field Size Measured by SRS MapCheck

As described earlier, the sensitivity of SRS MapCheck measurements to field size changes was measured by varying SDD from 750 to 850 mm with a step size of 10 mm. Because the Iris™ size R is proportional to the corresponding SSD: $R = R_0 * \text{SDD}/\text{SDD}_0$, where R_0 is the nominal Iris™ size at SDD_0 = 800 mm. The measured field sizes with the corresponding expected ones (the yellow lines) are presented in **Figure 7** for each of the cone sizes. A ±0.2 mm band centered at the expected Iris™ size is also added in the plot to aid visualization. **Figure 7** shows that for each Iris™ size, the measured field size changes linearly with the increase of the SDD. The fitting results showed a high coefficient of determination R^2 for each Iris™ size, increasing from 0.9814 to 0.9988 for Iris™ of 7.5 mm to 60 mm. The errors (the differences between the measured and the nominal scaled) were plotted in a scatter plot in **Figure 8(a)**. The histogram of the errors was also plotted in **Figure 8(b)** and fitted with a Gaussian. The Gaussian fit showed a mean difference $\mu = -0.009$ mm with $\sigma = 0.06$ mm. Thus, the measured Iris™ size using the SRS MapCheck had a standard error $\pm\Delta = \pm 1.96\ \sigma = \pm 0.12$ mm.

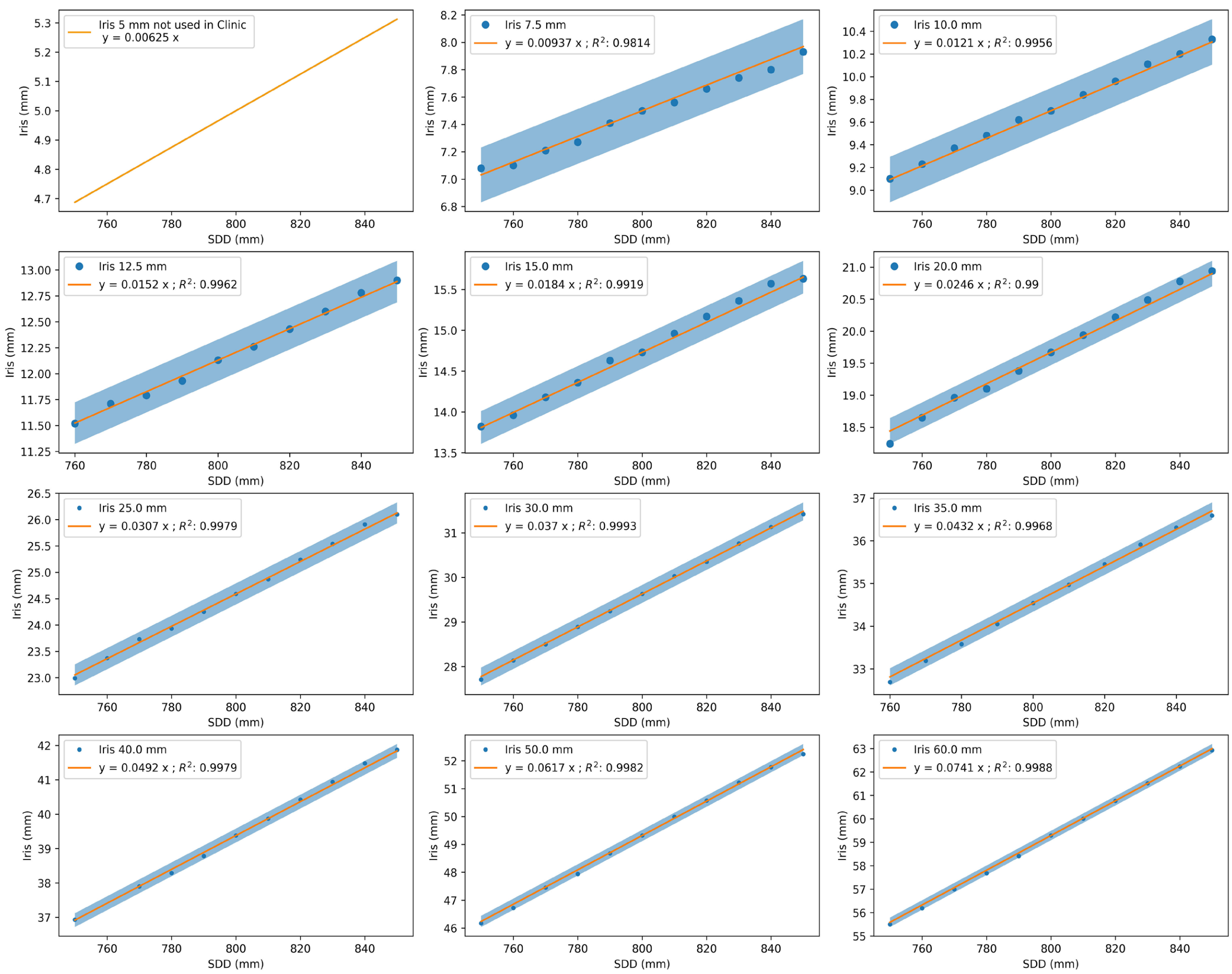

Figure 7. Example of a figure caption (figure caption). The Iris™ size of measured vs. nominal-scaled (the yellow line: $=R_0 * \text{SDD}/\text{SDD}_0$) with SDDs at 750, 780, 790, 800, 810, 820, and 850 mm respectively.

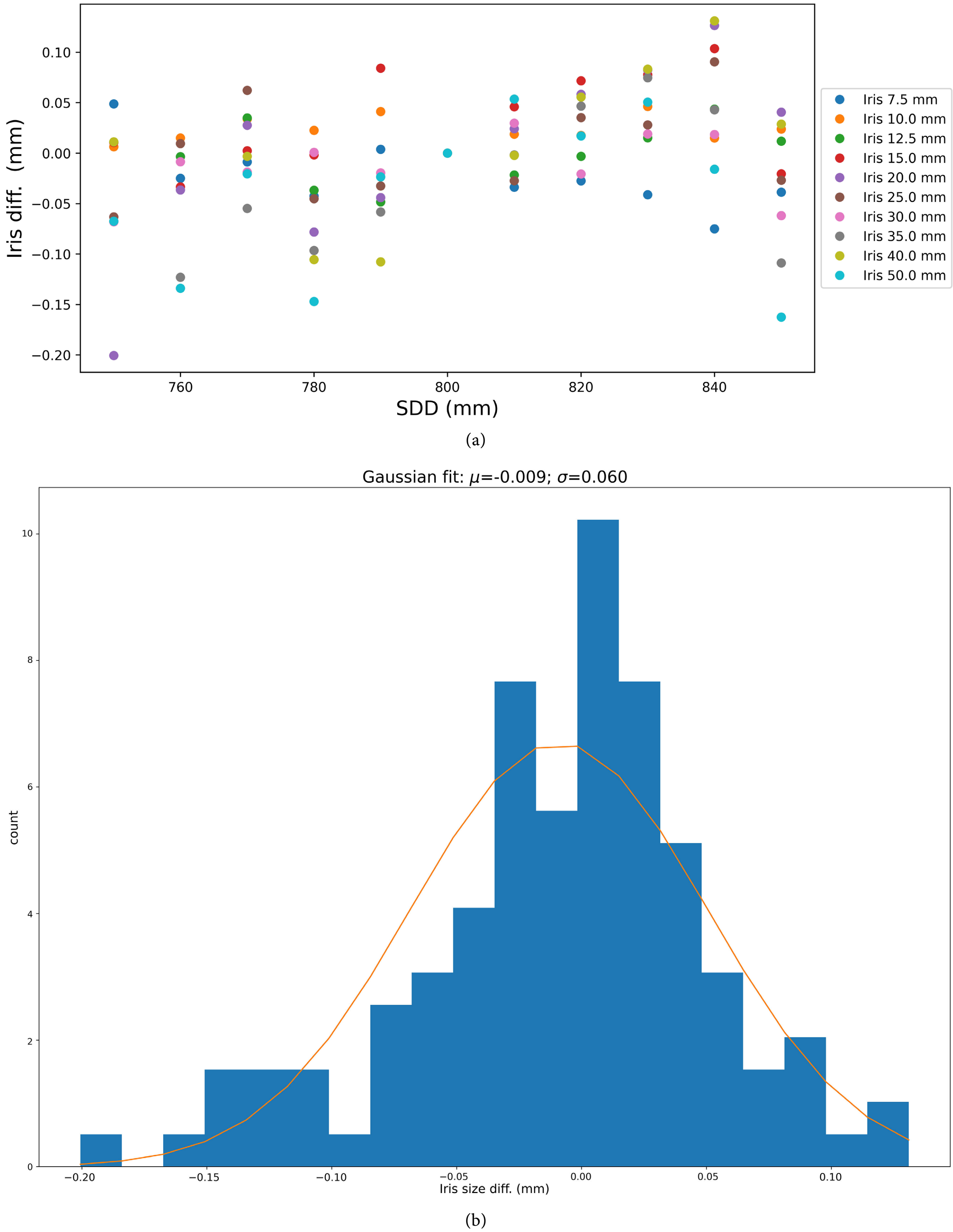

Figure 8. (a) The Iris™ size differences between the measured and the nominal scaled for all the cone sizes, with SDDs from 750 to 850 mm at a step size of 10 mm. (b) a Gaussian fit of the histogram of the Iris™ size measurement errors: ±0.12 mm.

4. Discussions

One important consideration when evaluating the suitability of the SRS MapCheck for the Iris™ QA is the Nyquist frequency of the dose profile being measured. The Nyquist frequency is a concept used in digital signal processing to determine the sampling rate required to accurately capture and reproduce a continuous signal. It relates to the highest frequency that can be correctly represented in a sampled signal without causing distortions or inaccuracies. According to the Nyquist-Shannon sampling theorem, we must sample at a rate that is at least twice the highest frequency component present in the signal. Because the spatial resolution of 0.4 mm^{-1} for the SRS MapCheck, its highest sampling frequency would be 0.2 mm^{-1}. However, the dose profiles have negligible contributions for frequency > 0.2 mm^{-1}, and our results showed the dose profile could still be reproduce with tolerable loss.

The ability to measure field size changes as small as 0.2 mm demonstrated the high sensitivity of the SRS MapCheck system, which is important for accurately detecting small changes in the intensity of the radiation beam where dose gradient could be as high as 10%/mm. It agrees with the reproducibility of the Iris™ field size being tested and validated to be less than or equal to 0.2 mm in our study. The cubic B-spline interpolation used by the SRS MapCheck system enables the reconstruction of dose profiles with high authenticity, even when the sampling resolution is only 2.5 mm. This is because the cubic B-spline interpolation is able to smooth out any irregularities in the measured data, resulting in a more accurate representation of the true dose distribution. Overall, the combination of the SRS MapCheck's high sensitivity and precision, along with its ability to accurately reconstruct dose profiles, makes it an effective tool for providing a consistent and high-precision monitoring of the CK Iris™ size.

In addition, one of the main advantages of the SRS MapCheck is its ability to significantly reduce the time required for QA compared to conventional film-based methods. In our study given, the measurement of 11 Iris™ cones took less than 10 minutes, with the setup being completed within 5 minutes and the delivery of all Iris™ beams within 3 minutes. The use of a customized QA plan and x-ray images to guide the alignment of the SRS MapCheck with four metal fiducials inside the device also contributes to the time-saving benefits of the SRS MapCheck. These features allow the system to be quickly and easily set up, reducing the time required for setup and preparation. By automating the switching of the Iris™ sizes, the system is able to more quickly and accurately deliver the various beams required for QA, further reducing the time required for the process.

Nevertheless, the applicability of SRS MapCheck in CK Monthly Iris™ QA is in agreement with its success in Linac QA [8], and the patient specific End-to-End QA [9] [10]. In patient QA, it has been shown applicable to perform Gamma analysis with tight criteria (e.g., 1 mm and 2%).

5. Conclusion

Our sensitivity study shows that the SRS MapCheck system is able to measure field sizes changes as small as 0.2 mm. Although the sampling resolution is only 2.5 mm, it has been shown sufficient for measuring CK Iris™ field sizes as these dose profiles were found to have few components with spatial frequency higher than 2 mm^{-1}. Moreover, the cubic B-spline interpolation enables the dose profile to be reconstructed with high authenticity. By and large, the SRS MapCheck provides a convenient and high-precision monitoring system for the CK Iris™ QA.

Conflicts of Interest

The authors declare no conflicts of interest regarding the publication of this paper.

References

[1] Nieder, C., Grosu, A.L. and Gaspar, L.E. (2014) Stereotactic Radiosurgery (SRS) for Brain Metastases a Systematic Review. *Radiation Oncology*, **9**, 155. https://doi.org/10.1186/1748-717X-9-155

[2] Solberg, T.D., Balter, J.M., Benedict, S.H., *et al.* (2012) Quality and Safety Considerations in Stereotactic Radiosurgery and Stereotactic Body Radiation Therapy: Executive Summary. *Practical Radiation Oncology*, **2**, 2-9. https://doi.org/10.1016/j.prro.2011.06.014

[3] Halvorsen, H., Cirino, E., Das, I.J., Garrett, J.A., Yang, J., Yin, F.F. and Fairobent, L.A., (2017) AAPM-RSS Medical Physics Practice Guideline 9.a. for SRS-SBRT. *Journal of Applied Clinical Medical Physics*, **18**, 10-21. https://doi.org/10.1002/acm2.12146

[4] Covington, E.L., Ritter, T.A., Moran, J.M., Owrangi, A.M. and Prisciandaro, J.I. (2016) Technical Report: Evaluation of Peripheral Dose for Flattening Filter Free Photon Beams. *Medical Physics*, **43**, 4789. https://doi.org/10.1118/1.4958963

[5] Budgell, G., Brown, K., Cashmore, J., Duane, S., *et al.* (2016) IPEM Topical Report 1: Guidance on Implementing Flattening Filter Free (FFF) Radiotherapy. *Physics in Medicine & Biology*, **61**, 8360-8394. https://doi.org/10.1088/0031-9155/61/23/8360

[6] Blanck, O., Masi, L., Chan, M.K., Adamczyk, S., Albrecht, C., Damme, M.C., *et al.* (2016) High Resolution Ion Chamber Array Delivery Quality Assurance for Robotic Radiosurgery: Commissioning and Validation. *Physics in Medicine & Biology*, **32**, 838-846. https://doi.org/10.1016/j.ejmp.2016.05.060

[7] Biasi, G., Petasecca, M., Guatelli, S., *et al.* (2018) CyberKnife((R)) Fixed Cone and Iris Defined Small Radiation Fields: Assessment with a High-Resolution Solid-State Detector Array. *Journal of Applied Clinical Medical Physics*, **19**, 547-557. https://doi.org/10.1002/acm2.12414

[8] Rose, M.S., Tirpak, L., Van Casteren, K., *et al.* (2020) Multi-Institution Validation of a New High Spatial Resolution Diode Array for SRS and SBRT Plan Pretreatment Quality Assurance. *Medical Physics*, **47**, 3153-3164. https://doi.org/10.1002/mp.14153

[9] Ahmed, S., Zhang, G., Moros, E.G. and Feygelman, V. (2019) Comprehensive Evaluation of the High-Resolution Diode Array for SRS Dosimetry. *Journal of Applied Clinical Medical Physics*, **20**, 13-23. https://doi.org/10.1002/acm2.12696

[10] Xu, Q., Huynh, K., Nie, W., Rose, M.S., *et al.* (2022) Implementing and Evaluating a High-Resolution Diode Array for Patient-Specific Quality Assurance of Robotic

Brain Stereotactic Radiosurgery/Radiotherapy. *Journal of Applied Clinical Medical Physics*, **23**, e13569. https://doi.org/10.1002/acm2.13569